

# A Single-Step Multiclass SVM based on Quantum Annealing for Remote Sensing Data Classification

Amer Delilbasic, *Student Member, IEEE*, Bertrand Le Saux, *Senior Member, IEEE*, Morris Riedel, *Member, IEEE*, Kristel Michielsen, and Gabriele Cavallaro, *Member, IEEE*

**Abstract**—In recent years, the development of quantum annealers has enabled experimental demonstrations and has increased research interest in applications of quantum annealing, such as in quantum machine learning and in particular for the popular quantum SVM. Several versions of the quantum SVM have been proposed, and quantum annealing has been shown to be effective in them. Extensions to multiclass problems have also been made, which consist of an ensemble of multiple binary classifiers. This work proposes a novel quantum SVM formulation for direct multiclass classification based on quantum annealing, called Quantum Multiclass SVM (QMSVM). The multiclass classification problem is formulated as a single Quadratic Unconstrained Binary Optimization (QUBO) problem solved with quantum annealing. The main objective of this work is to evaluate the feasibility, accuracy, and time performance of this approach. Experiments have been performed on the D-Wave Advantage quantum annealer for a classification problem on remote sensing data. The results indicate that, despite the memory demands of the quantum annealer, QMSVM can achieve accuracy that is comparable to standard SVM methods and, more importantly, it scales much more efficiently with the number of training examples, resulting in nearly constant time. This work shows an approach for bringing together classical and quantum computation, solving practical problems in remote sensing with current hardware.

**Index Terms**—Support Vector Machine (SVM), Quantum Computing (QC), Quantum Annealing (QA), classification, Remote Sensing (RS)

## I. INTRODUCTION

**I**N the context of Earth Observation (EO) [1], there is a growing availability of data acquired by heterogeneous Remote Sensing (RS) sources. Many applications are currently benefitting from RS data, e.g., agriculture, green energy development and urban monitoring. The devices and software for data processing have to match this trend in order to extract information from the collected data in a timely manner.

Amer Delilbasic is with the Jülich Supercomputing Centre, Wilhelm-Johnen Straße, 52428 Jülich, Germany, with the University of Iceland, 107 Reykjavik, Iceland, and with ESA/ESRIN  $\Phi$ -lab, IT-00044 Frascati, Italy (e-mail: a.delilbasic@fz-juelich.de).

Bertrand Le Saux is with ESA/ESRIN  $\Phi$ -lab, IT-00044 Frascati, Italy (e-mail: bertrand.le.saux@esa.int).

Morris Riedel and Gabriele Cavallaro are with the University of Iceland, 107 Reykjavik, Iceland, and the Jülich Supercomputing Centre, Wilhelm-Johnen Straße, 52428 Jülich, Germany (e-mail: morris@hi.is, g.cavallaro@fz-juelich.de).

Kristel Michielsen is with the Jülich Supercomputing Centre, Wilhelm-Johnen Straße, 52428 Jülich, Germany, and the RWTH Aachen University, D-52056 Aachen, Germany (e-mail: k.michielsen@fz-juelich.de).

This work has been submitted to the IEEE for possible publication. Copyright may be transferred without notice, after which this version may no longer be accessible.

Quantum Computing (QC) [2], a computational paradigm based on the postulates and laws of quantum mechanics, has proved the potential to reach an exponential algorithmic speedup with respect to classical computation under certain assumptions [3], [4]. Among the quantum computational models defined in the literature, two broadly employed models can be identified. The quantum circuit model [5], similarly to the classical circuit model, is based on circuits, gates and measurements applied to qubits (quantum bits). Adiabatic Quantum Computation (AQC) [6], [7] aims at solving optimization problems by exploiting the time evolution of a quantum system satisfying the requirements of the adiabatic theorem [8]. Despite their differences, the two models have been proven to be computationally equivalent [9]. The focus of this work is Quantum Annealing (QA) [10], [11], a heuristic search approach based on AQC, since commercially ready quantum annealers are available for analyzing the disruptive potential of QC.

Quantum Machine Learning (QML) [12], [13] is a research area working on QC algorithms applied to Machine Learning (ML) tasks, with the purpose of obtaining a computational speedup or a prediction accuracy increase. QML methods based on QA have proven to outperform classical ML in selected applications with limited training examples, for example in computational biology [14]. Recent studies have analyzed how QML can be integrated into EO tasks. In [15] and [16], circuit-based quantum neural networks have been trained for multispectral image classification. The work of Otgonbaatar and Datcu has covered different aspects of circuit-based QML for EO, e.g., natural data embedding [17], parameterized quantum gates [18] and transfer learning [19]. Circuit-based quantum kernels have been applied to binary [20] and multiclass [21] RS image classification. QA has also found a place in EO for solving specific optimization problems. In Synthetic Aperture Radar (SAR) imaging, problems related to system design [22] and phase ambiguity [23] have been addressed. In the context of QML, a feature selection method for hyperspectral images has been proposed [24], and a QA-based Quantum SVM (QSVM) method has been successfully used for binary classification of multispectral images [25] [26].

The Support Vector Machine (SVM) is an efficient and theoretically-grounded algorithmic approach in statistical learning theory. Different versions and formulations of the SVM can be found in the literature for a variety of tasks and applications, e.g., pattern recognition, computer vision, image analysis and business intelligence [27]. SVM has also been proven to be effective in EO pixel-wise image classification

[28].

Defining a SVM framework for multiclass classification is a non-trivial task. Two different approaches can be followed [29]. The *multiple-step* (or *indirect*) *approach* reframes the problem by defining an ensemble of multiple binary SVM classifiers and multiple classification outputs. The most common methods are the one-versus-one (OVO), one-versus-all (OVA) and the Directed Acyclic Graph (DAG) SVM. In the OVO method, for example, each pair of classes defines a SVM classifier. The outcomes of each classifier are usually combined with a “max wins” strategy which determines the final prediction. The QSVM algorithms for multiclass classification available in the literature, e.g., [30], [31], [32], follow this approach. They are defined as ensembles of binary QSVM classifiers, which can be full quantum [33], [34], quantum kernel [35] and QA-based [36] formulations.

The *single-step* (or *direct*) *approach* for multiclass classification defines a single optimization step on the whole training set, which finds boundaries between all classes in one pass. The Crammer-Singer (CS) SVM, proposed in [37], is an example of single-step approach. A limitation of this method is the complexity of the training phase, due to the high number of optimization variables, which makes this approach impractical. In the same work, simplified formulations are proposed, which reduce the problem size and enable better performances, although at the cost of optimality.

The main objective of this work is to propose a novel approach, specifically Quantum Multiclass SVM (QMSVM), by reframing the original formulation of the CS SVM, thus enabling the optimization step to be performed using a QA algorithm. This work studies the computational capability offered by the available quantum annealers and test the feasibility of a QA-based SVM single-step approach. Experiments are performed on a real quantum annealer, i.e., D-Wave Advantage [38], [39], in order to validate the algorithm and analyze the potential of current hardware. The performance is evaluated both in terms of accuracy and execution time, both relevant aspects in practice. The code repository of the algorithm is made available for reproducibility<sup>1</sup>.

## II. BACKGROUND

### A. Quantum Annealing and QUBO

To understand the underlying working principles of D-Wave quantum annealers, a brief introduction is needed. In AQC [6], [7], the forces acting in a quantum system are described by a time-varying Hamiltonian  $\mathcal{H}(t)$ . The time evolution of the state of a quantum system  $|\varphi(t)\rangle$  is described by the Schrödinger’s Equation:

$$i\hbar \frac{\partial |\varphi(t)\rangle}{\partial t} = \mathcal{H}(t) |\varphi(t)\rangle \quad (1)$$

where  $i$  is the imaginary unit and  $\hbar$  is the reduced Planck constant. During the adiabatic evolution, the Hamiltonian gradually transitions from the initial Hamiltonian  $\mathcal{H}_I$  to the final Hamiltonian  $\mathcal{H}_F$ :

$$\mathcal{H}(t) = s(t)\mathcal{H}_I + (1 - s(t))\mathcal{H}_F \quad (2)$$

where  $s(t)$  is a function modeling the transition, such that  $s(0) = 1$  and  $s(t_f) = 0$  after a certain elapsed time  $t_f$ . Given the assumptions of the adiabatic theorem [8], during the time evolution, the quantum system remains at ground state, i.e., the state with lowest energy associated with the Hamiltonian. The idea in AQC is to encode the desired result as the ground state of the final Hamiltonian  $\mathcal{H}_F$ .

QA falls into the category of AQC algorithms. More precisely, it is a heuristic approach for solving combinatorial optimization problems. In this case, the Hamiltonian of the system is defined as:

$$\mathcal{H}(t) = \mathcal{H}_F + \Gamma(t)\mathcal{H}_D \quad (3)$$

where  $\mathcal{H}_F$  is the final Hamiltonian,  $\Gamma(t)$  is the *transverse field coefficient* as a function of time  $t$ , and  $\mathcal{H}_D$  is the *transverse field Hamiltonian* (also called *disorder Hamiltonian*).  $\mathcal{H}_F$  encodes the objective function and its ground state is the solution of the optimization problem.  $\Gamma(t)$  is a decreasing function, equal to 0 for  $t = t_f$ . It controls the contribution of  $\mathcal{H}_D$ , which enables traversibility of the solution space, making the optimization process escape local minima. As for this aspect, QA presents a similarity with simulated annealing [40], where the temperature parameter  $T$  resembles the role of  $\Gamma(t)$ . In this framework, the assumptions of the adiabatic theorem are relaxed, i.e., there is no requirement for the quantum system to be closed and to operate in the ground state. The implementation of QA provided by D-Wave quantum annealers enables the solution of a specific type of optimization problems, called Quadratic Unconstrained Binary Optimization (QUBO) problems. A QUBO problem is defined as:

$$\text{minimize} \quad \sum_{i < j} a_i Q_{ij} a_j \quad (4)$$

where  $a_i \in \{0, 1\}$  are the binary variables of the problem and  $Q$  an upper-triangular matrix called QUBO matrix.

### B. Minor Embedding

Some restrictions on the QUBO problems submitted to D-Wave quantum annealers are enforced, which are related to the physical qubit architecture. The qubit connectivity parameter describes how many physical connections, i.e., couplers, are implemented for each qubit. D-Wave Advantage is based on the Pegasus architecture and presents approximately 5000 qubits, 35000 couplers and a qubit connectivity of 15 [39]. When the QUBO problem is submitted to a quantum annealer, a step called *minor embedding* [41] is performed. In the minor embedding step, a qubit chain is assigned to each binary variable of the problem  $a_i$ . The main requirement is maintaining the logical structure of the problem, described by  $Q$ . Each element of the QUBO matrix  $Q_{ij}$  represents a logical relation between the variables  $a_i$  and  $a_j$ . The coefficients  $Q_{ij}$  are mapped to the strength of the couplers connecting the qubit chains assigned to the variables  $a_i$  and  $a_j$ . The existence of such an embedding is a requirement for a problem to be solved by the annealer, i.e., constraints on the dimension and the structure of the QUBO problem need to be satisfied. In Fig. 1, the embedding of a QUBO problem in graph form is shown.

<sup>1</sup><https://gitlab.jsc.fz-juelich.de/sdlrs/qmsvm>

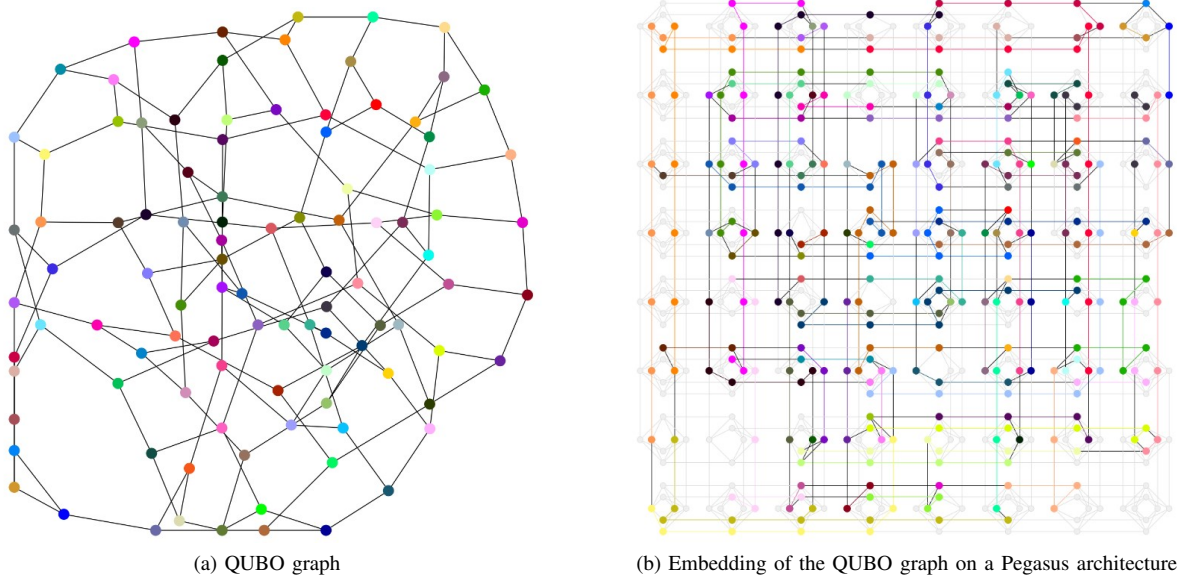


Fig. 1. Graphical representation of the minor embedding step. In the graph shown in (a), each node represents a binary variable and each edge represents a logical connection between two variables of the QUBO problem. In (b), each qubit chain is defined by the color of the embedded variable. Source: [6]

### III. QUANTUM MULTICLASS SVM FORMULATION

In this section, a novel algorithm called QMSVM is described. It is based on a reformulation of the Crammer-Singer (CS) SVM [37] as a QUBO problem. The followed steps are adapted from the QSVM proposed in [36], with the addition of a solution combination method. As a starting point, the CS SVM formulation is described in the following.

#### A. Crammer-Singer Multiclass SVM

In a supervised multiclass classification problem, let  $N$  be the number of training examples,  $C$  the number of classes,  $X^{tr} = \{\mathbf{x}_n\}$  the feature vectors of dimension  $F$ ,  $Y^{tr} = \{y_n\}$  the labels. The training consists in the solution of the following quadratic program:

$$\begin{aligned} \text{minimize } F(T) &= \frac{1}{2} \sum_{n_1, n_2=0}^{N-1} K(\mathbf{x}_{n_1}, \mathbf{x}_{n_2}) \sum_{c=0}^{C-1} \tau_{n_1 c} \tau_{n_2 c} \\ &\quad - \beta \sum_{n=0}^{N-1} \sum_{c=0}^{C-1} \delta_{c y_n} \tau_{n c} \\ \text{subject to } \sum_{c=0}^{C-1} \tau_{n c} &= 0 \quad \forall n, \quad \tau_{n c} \leq 0 \quad \forall n, \forall c \neq y_n. \end{aligned} \quad (5)$$

where  $T = [\tau_{nc}]$  is the matrix of the  $NC$  problem variables, with  $n = 0, \dots, N-1$ ,  $c = 0, \dots, C-1$  and  $\tau_{nc} \in [-1, 1]$ ,  $\delta_{ij}$  is the Kronecker delta and  $\beta$  a regularization parameter.

D-Wave Advantage is unable to directly solve Eq. (5)-(6). Therefore, a reformulation of Eq. (5)-(6) as a QUBO problem is necessary. The followed steps are: choosing a binary encoding (Sect. III-B), defining the penalty terms (Sect. III-C), deriving the QUBO matrix including the results of the previous steps in the cost function (Sect. III-D), and defining a solution combination method (Sect. III-E).

#### B. Binary Encoding

The first step consists in defining the binary variables  $a_i$  of the QUBO problem. In the CS formulation, the problem variables  $\tau_{nc}$  are real numbers. The idea is to discretize the solution space using uniform sampling and represent each value as a set of  $B$  binary variables. First, the following intermediate variable is defined:

$$\sigma_{nc} = \sum_{b=0}^{B-1} 2^b a_{nCB+cB+b}. \quad (7)$$

$\sigma_{nc}$  is an integer value in  $[0, 2^B - 1]$  represented by the binary encoding  $\{a_{nCB+cB+b}, b = 0, \dots, B-1\}$ . Then, the problem variables  $\tau_{nc}$  can be defined from  $\sigma_{nc}$  as:

$$\tau_{nc} = -1 + \frac{2}{2^B - 1} \sigma_{nc} = -1 + \frac{2}{2^B - 1} \sum_{b=0}^{B-1} 2^b a_{nCB+cB+b}. \quad (8)$$

With this definition, it can be proven that each value of  $\tau_{nc}$  lies in  $[-1, 1]$  and the interval is uniformly sampled.

Fig. 3 shows the sampling of Eq. (8) for  $B = 2$ , i.e., in the case each sample of  $\tau_{nc}$  is represented by 2 binary variables, indicated above each sample. Since the total number of problem variables is  $NC$  (each variable is associated with an example and a class), the whole optimization space can be represented by a set of  $NCB$  binary variables  $\{a_0, a_1, \dots, a_{NCB-1}\}$ .

#### C. Penalty Terms

Another requirement is to include the constraints of Eq. (6), as no constraints can be directly enforced in a QUBO problem. A possibility is to add the constraints to the QUBO matrix as weighted positive penalty terms. For the first constraint,

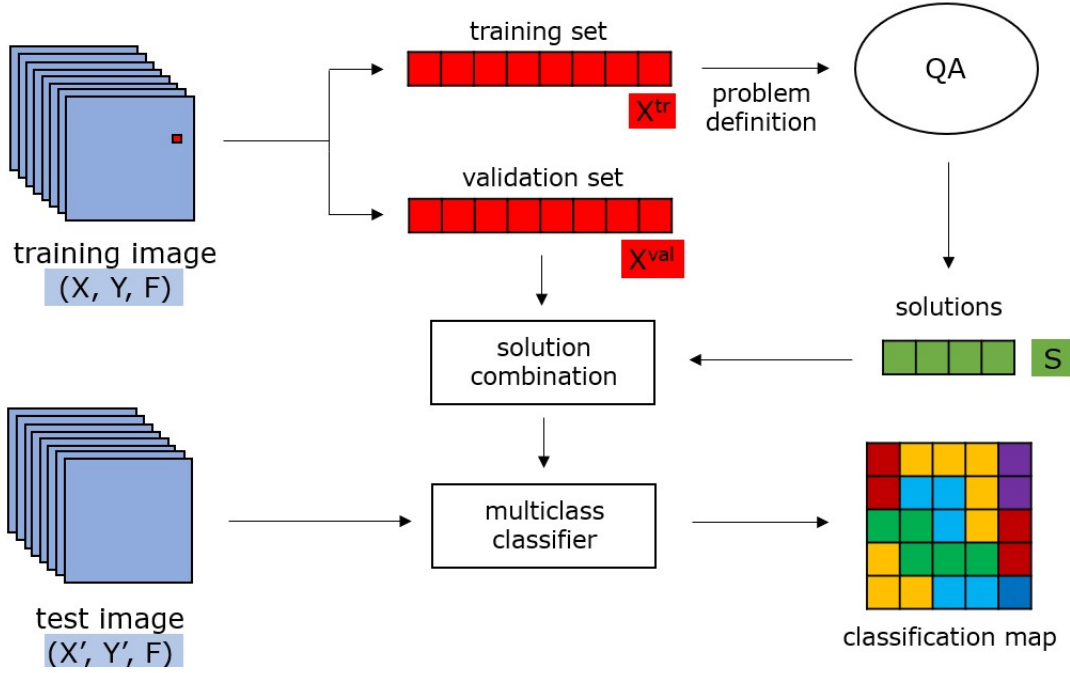


Fig. 2. Workflow for the QMSVM algorithm. A training set  $X^{tr}$  is given as input to the QA step, which obtains a set of  $S$  solutions to the training problem. The solutions are then combined according to the accuracy performance on a validation set  $X^{val}$ , to generate the final classifier.

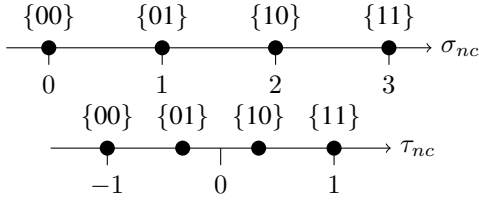


Fig. 3. Representation of the chosen variable sampling and encoding for  $B = 2$ .

the penalty term needs to increase in the case the difference between the value of the sum and 0 increases. In addition, a penalty term needs to be associated with each training example and with the same weight. Since a quadratic polynomial term is required, the following penalty term is chosen:

$$P_n^1 = \left( \sum_{c=0}^{C-1} \tau_{n,c} \right)^2 \quad (9)$$

For the second constraint, which is an inequality, it is sufficient to directly consider  $\tau_{nc}$  as the penalty term associated with each training sample and each class. A coefficient  $(1 - \delta_{cy_n})$  is attached to account for the case  $c = y_n$ , in which the penalty is zero:

$$P_{nc}^2 = (1 - \delta_{cy_n}) \tau_{n,c} \quad (10)$$

The final penalty term can be written as:

$$\begin{aligned} P &= \sum_{n=0}^{N-1} P_n^1 + \sum_{n=0}^{N-1} \sum_{c=0}^{C-1} P_{nc}^2 \\ &= \sum_{n=0}^{N-1} \left( \sum_{c=0}^{C-1} \tau_{n,c} \right)^2 + \sum_{n=0}^{N-1} \left( \sum_{c=0}^{C-1} (1 - \delta_{cy_n}) \tau_{n,c} \right) \end{aligned} \quad (11)$$

Note that  $P_n^1$  and  $P_{nc}^2$  are included with the same weight. The following reasons behind this choice can be listed:

- Considering two different weights would increase the number of hyperparameters of the optimization problem and the already high complexity of the tuning phase;
- The two constraints have to be both equally satisfied;
- The two penalty terms have approximately the same order of magnitude, as  $\tau_{nc} \in [-1, 1]$ , so there is no imbalance in values.

#### D. QUBO Matrix

The QUBO problem can be now written by adding to Eq. (5) the penalty term in Eq. (11) multiplied by a weight  $\mu$  and substituting  $\tau_{i,j}$  with the encoding in Eq. (8). The energy function  $E$  can be written in the following form<sup>2</sup>:

$$E = F + \mu P = \sum_{n_1 n_2 c_1 c_2 b_1 b_2} a_{n_1 c_1 B + c_1 B + b_1} \tilde{Q}_{n_1 c_1 B + c_1 B + b_1, n_2 c_2 B + c_2 B + b_2} a_{n_2 c_2 B + c_2 B + b_2} \quad (12)$$

$\tilde{Q}$  is a symmetric matrix of size  $NCB \times NCB$ . It can be analytically derived by neglecting the terms not depending on

<sup>2</sup>In this formulation, a simplified notation for the sums is used, as the range of the indices is unaltered and redundant.

the binary variables and is equal to:

$$\begin{aligned} & \tilde{Q}_{n_1 c B + c_1 B + b_1, n_2 c B + c_2 B + b_2} = \\ & = \delta_{n_1 n_2} \delta_{c_1 c_2} \delta_{b_1 b_2} \frac{2^{b_1+1}}{2^B - 1} \left( - \sum_i K(\mathbf{x}_{n_1}, \mathbf{x}_i) \right. \\ & \quad \left. - \delta_{c_1 y_{n_1}} (\beta + \mu) - 2C\mu + \mu \right) \\ & \quad + \delta_{c_1 c_2} \frac{2^{b_1+b_2+1}}{(2^B - 1)^2} K(\mathbf{x}_{n_1}, \mathbf{x}_{n_2}) + \delta_{n_1 n_2} \frac{2^{b_1+b_2+2}\mu}{(2^B - 1)^2} \end{aligned} \quad (13)$$

The upper-triangular QUBO matrix  $Q$  can be computed from  $\tilde{Q}$  as:

$$Q_{ij} = \begin{cases} \tilde{Q}_{ij} & \text{for } i = j \\ \tilde{Q}_{ij} + \tilde{Q}_{ji} & \text{for } i < j \\ 0 & \text{otherwise} \end{cases} \quad (14)$$

### E. Solution Combination

Once the QUBO matrix is defined, the problem can be submitted to the quantum annealer, assuming the existence of an embedding. As the annealing process is performed multiple times, depending on the value of  $num\_reads$ , the obtained output is a set of  $num\_reads$  solutions. The best  $S$  solutions are selected, i.e.,  $T_i = [\tau_{nc}]_i, i = 0, \dots, S-1$ , ranked by the value of the energy function  $E(T_i)$ . During the experiments, it has been noticed that there is no perfect correlation between solutions with lower energy and better classification accuracy of the obtained classifier. Note also that the solution space investigated by the quantum annealing algorithm is discrete, due to the variable sampling, so the obtained individual solutions can be sub-optimal. For these reasons, a solution combination is performed in order to obtain an optimal final solution. A weighted average is performed, where the weights  $w_s$  for each solution  $s$  are set according to the prediction accuracy of the obtained classifiers on a validation set  $\{X^{val}, Y^{val}\}$ . In particular, the solutions above a certain threshold accuracy are selected, and their weight is computed applying the softmax function to  $multiplier \cdot accuracy_s$ , where  $multiplier$  is a real value and  $accuracy_s$  is the accuracy of the classifier defined by the  $s$ -th solution on the whole training set. The rest of the weights are set to 0. The combined solution is computed as:

$$\bar{T} = \frac{1}{S} \sum_{s=0}^{S-1} w_s T_s. \quad (15)$$

The resulting variables  $\bar{\tau}_{nc}$  are then used to classify new examples:

$$H(\mathbf{x}) = \arg \max_c \left\{ \sum_{n=0}^{N-1} \bar{\tau}_{nc} K(\mathbf{x}, \mathbf{x}_n) \right\} \quad (16)$$

Alg. 1 summarizes the implemented computational steps required for the training.

## IV. EVALUATION

### A. Experimental Setup

The QMSVM algorithm has been validated on a semantic segmentation problem applied to multispectral RS images.

### Algorithm 1 Quantum Multiclass SVM (QMSVM)

**Input:**  $X^{tr}, Y^{tr}, X^{val}, Y^{val}, C, B, \beta, \mu, \gamma, S$ , multiplier

**Output:**  $\bar{T}$

- 1:  $Q \leftarrow$  QUBO\_MATRIX( $X^{tr}, Y^{tr}, C, B, \beta, \mu, \gamma$ )
- Run annealing step and sample  $num\_reads$  solutions
- 2:  $T \leftarrow$  QUANTUM\_ANNEALING( $Q$ )
- Evaluate classifier on validation set, eq. (16)
- 3: **for**  $s = 1$  to  $S$  **do**
- 4:  $\hat{Y}^{val}[s] \leftarrow H(X^{val}, Y^{val}, T)$
- 5:  $accuracy[s] \leftarrow$  ACCURACY( $\hat{Y}^{val}[s], Y^{val}$ )
- 6: **end for**
- Weights calculation
- 7:  $threshold \leftarrow$  THRESHOLD( $accuracy$ )
- 8: **for**  $s = 1$  to  $S$  **do**
- 9: **if**  $accuracy[s] < threshold$  **then**
- 10:  $accuracy[s] \leftarrow 0$
- 11: **end if**
- 12: **end for**
- 13:  $W \leftarrow$  SOFTMAX( $multiplier \cdot accuracy$ )
- Solution combination, eq. (15)
- 14:  $\bar{T} \leftarrow$  COMBINE( $T, W$ )
- 15: **return**  $\bar{T}$

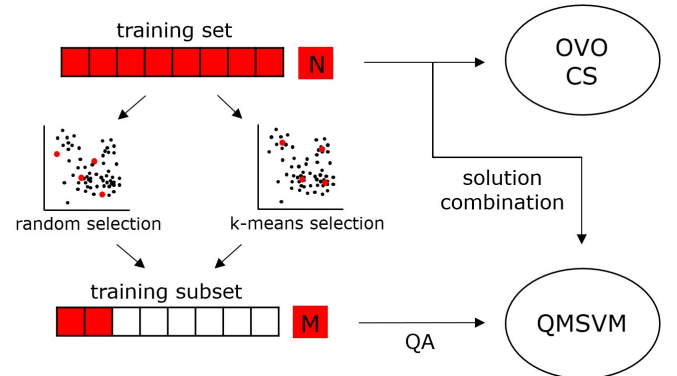


Fig. 4. Training setup. The OVO and CS methods have been trained on a training set of  $N$  examples. For QMSVM, a subset of  $M$  examples is selected and used by the annealing algorithm, while the solution combination is performed based on the accuracy obtained on the whole training set.

Two different datasets are considered, i.e., SemCity Toulouse [42] (hereafter “Toulouse”) and ISPRS Potsdam [43] (hereafter “Potsdam”). Tab. I describes the selected datasets. While both represent urban areas, the two datasets differ in the used features and the ground resolution. From each dataset, a training set of  $N$  examples is initialized.

The experiments have been performed on a real quantum device, JUPSI [44], a D-Wave Advantage quantum annealer located at Forschungszentrum Jülich. The *Advantage\_system5.3* cloud solver has been used. Given the memory and connectivity limitation of the machine, the training set  $\{X^{tr}, Y^{tr}\}$  defined in Sect. III-A is initialized as a subset of  $M$  examples from the total number of training examples  $N$ . The training subset is computed through an example selection step, and two selection methods have been tested.

TABLE I  
DATASETS USED IN THE EXPERIMENTS.

Dataset	Dimension	Resolution	Features	Classes	Training Set	Test Set
SemCity Toulouse [42]	16 tiles, $3504 \times 3452$	2 m	8 bands	7	$N$ samples, tile 4	$800 \times 800$ area, tile 8
ISPRS Potsdam [43]	38 tiles, $6000 \times 6000$	5 cm	4 bands + DSM	5	$N$ samples, Tile 6_9	$1000 \times 1000$ area, tile 6_10

TABLE II  
PARAMETERS SETUP.

Variable Name	Value	Description
$C$	3	Number of classes considered in the multiclass classification problem
$B$	2	Number of binary variables representing each problem variable $\tau_{nc}$
$\beta$	1	Model related regularization parameter, introduced in Eq. (5)
$\mu$	1	Weight of the penalty term $P$ added to the energy function defined in Eq. (12)
$\gamma$	1	Gaussian kernel parameter, regulating its radius
$N$	[50, 40000]	Total number of training examples used in the training (multiple values analyzed)
$M$	60	Number of selected training examples, used to define the QUBO matrix $Q$ submitted to the QA
$num\_reads$	1000	Number of times the annealing schedule is performed and how many solutions are sampled for each run
$S$	100	Number of solutions selected among the total number $num\_reads$ , used for the solution combination
$multiplier$	10	Regulates the balance between higher and lower accuracy values over the combined solutions
$max\_min\_ratio$	15	Ratio between the maximum and minimum non-zero absolute value of the QUBO matrix $Q$
$chain\_strength$	1	Relative coupling strength between qubits that form a chain and qubits in different chains
$annealing\_time$	200	Time (in $\mu s$ ) at which the measurement is performed after starting the annealing schedule

- *Random selection*:  $M$  random examples are selected from the whole training set. It is a fast and straightforward method, enforcing no selection criterion.
- *K-means selection*: k-means clustering [45] is applied to each of the  $C$  classes, with  $k = \frac{M}{C}$ , and the obtained  $M$  centroids are used as selected examples. It is inspired by undersampling techniques in imbalanced classification [46]. In principle, the method is designed to select meaningful examples, covering the whole feature domain.

The whole training set is then used as the validation set  $\{X^{val}, Y^{val}\}$  for the solution combination, introduced in Sect. III-E. The *threshold* accuracy, which determines which solutions are discarded in the combination, has been computed as:

$$threshold = 0.2 \cdot \min(accuracy) + 0.8 \cdot \max(accuracy). \quad (17)$$

The results are compared with two standard implementations of the Multiclass SVM (MSVM), i.e., the OVO implementation in Scikit-learn [47] and a CS SVM implementation in C++ [48]. The training setup is depicted in Fig. 4.

## B. Parameters

In Tab. II the parameters of the problem are described. The parameters  $\beta$ ,  $\mu$  and  $\gamma$  are set through a simple grid search optimization on a validation set. Different values of  $N$  are chosen in order to analyze the performance of the method by varying the number of available examples. The highest tested value is  $N = 40000$  for Toulouse and  $N = 15000$  for Potsdam. The parameters  $B$ ,  $M$  and  $max\_min\_ratio$  are related to the main limitation of the QA, i.e., the number of qubits and couplers. As previously discussed, the possibility of finding an embedding on the given qubit architecture is

TABLE III  
RESULTS OF ACCURACY, F1 SCORE AND EXECUTION TIME FOR OVO AND QMSVM.

Solver	N	M	Accuracy	F1	t (s)
<i>Toulouse - best accuracy, maximum N</i>					
OVO	40000	-	0.9123	0.9147	726.49
CS	40000	-	0.8277	0.8463	2951.18
QMSVM (random)	40000	60	0.8803	0.8881	125.76
QMSVM (k-means)	40000	60	0.8406	0.8483	168.36
<i>Potsdam - best accuracy, maximum N</i>					
OVO	15000	-	0.8556	0.8599	808.37
CS	15000	-	0.8226	0.8362	2708.62
QMSVM (random)	15000	60	0.7814	0.7880	95.72
QMSVM (k-means)	15000	60	0.7648	0.7640	74.36

required for solving the QUBO problem. This is achieved in case  $Q$  is sufficiently small, sufficiently sparse, or both. Using only the selected training subset, the dimension of  $Q$  is  $MCB$ . Thus,  $M$  is limited, which is the reason the QA is unable to use an arbitrarily large training set and the example selection is performed in the first place. To maximize the number of examples fitting in the QA, the remaining parameters are kept low, i.e.,  $C = 3$  and  $B = 2$ . Considering a higher number of classes, i.e.,  $C > 3$ , would require using a lower number of examples  $M$ , which degrades the overall performance. Regarding sparsity, a straightforward operation is performed, i.e., pruning the values of  $Q$  below the threshold defined by  $max\_min\_ratio$ . This simplification is acceptable, as relatively low values would be mapped to relatively low strengths in the QA, which barely affect the annealing process. The parameters  $num\_reads$ ,  $chain\_strength$  and  $annealing\_time$  are related to

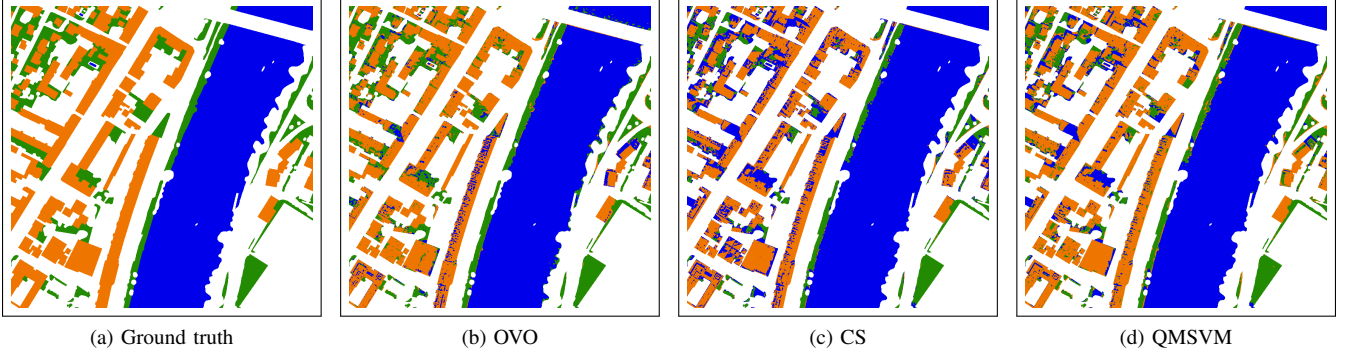


Fig. 5. Toulouse - ground truth and predicted land cover maps on an  $800 \times 800$  selected area from tile 8 for one-versus-one (OVO), Crammer-Singer (CS) and Quantum Multiclass SVM (QMSVM) using  $N = 40000$  training examples. The considered classes are "building" (orange), "pervious surface" (green) and "water" (blue).

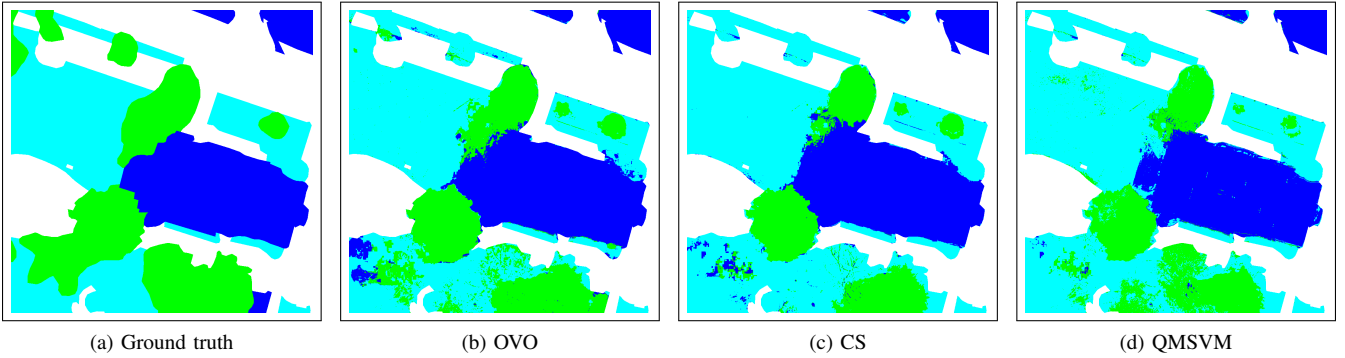


Fig. 6. Potsdam - ground truth and predicted land cover maps on a  $1000 \times 1000$  selected area from tile 6\_10 for one-versus-one (OVO), Crammer-Singer (CS) and Quantum Multiclass SVM (QMSVM) using  $N = 15000$  training examples. The considered classes are "building" (blue), "low vegetation" (light blue) and "tree" (green).

the annealer setup. Their values are chosen considering the impact they have on the quality of the obtained solutions [49]. The remaining parameters are set arbitrarily. Tab. II summarizes the chosen parameter values.

### C. Results

In the test phase, the methods are evaluated on a 3-class classification problem on a subtile. For Toulouse, a  $800 \times 800$  test subtile from tile 8 has been selected and the classes "building", "pervious surface", "water" have been considered. For Potsdam, a  $1000 \times 1000$  test subtile from tile 6\_10 has been selected and the classes "building", "low vegetation", "tree" have been considered.

The method is evaluated according to both test accuracy and execution time. For OVO and CS, training and inference are considered. For QMSVM, the time measurement includes preprocessing (sample selection), training (annealing), post-processing (solution combination) and inference time. Fig. 5-6 shows the ground truth of the selected subtile and the ground maps obtained by OVO, CS and QMSVM. In Fig. 7-10 the performance of the analyzed methods on the Toulouse and Potsdam dataset is shown in terms of both test accuracy and execution time, and for both example selection methods, i.e., random and k-means selection. Tab. III summarizes the

best obtained results in terms of test accuracy, along with the respective  $F_1$  score. Accuracy and  $F_1$  score are computed as:

$$\text{accuracy} = \frac{\text{correct predictions}}{\text{no. of predictions}}, \quad F_1 = \text{average}_c(F_{1c}). \quad (18)$$

$F_{1c}$  is the  $F_1$  score computed for each class  $c$  with respect to the remaining classes:

$$F_{1c} = \frac{\text{TP}_c}{\text{TP}_c + \frac{1}{2}(\text{FN}_c + \text{FP}_c)}, \quad (19)$$

where TP (true positive), FN (false negative) and FP (false positive) predictions are referred to the class  $c$ . Given the result variability for QMSVM, related to the intrinsic randomness of the example selection, 5 runs for each selection method have been performed, each one with a different chosen random seed. For each selection method, the average result is plotted and the space between the best and the worst obtained result is highlighted.

### D. Analysis

From a first impression, it can be noticed that QMSVM is a feasible quantum implementation of the CS SVM method. QMSVM is able to reach a slightly lower or comparable classification accuracy with respect to CS, despite the low

number of training examples  $M$  that can handle in the optimization step. The reason is that the solution combination using  $N$  examples is able to improve the quality of the final solution on average by increasing  $N$ , as seen in the accuracy plots. However, the prediction accuracy of OVO is slightly higher than both CS and QMSVM for higher  $N$ . A worse performance of QMSVM can be clearly seen on the more complex Potsdam dataset, where the result variability is also higher with respect to Toulouse. In both cases, the random selection method consistently outperforms k-means selection.

Regarding the execution time, QMSVM can better handle a high number of training examples  $N$  with respect to OVO and CS. The different steps included in the measurement of the execution time are shown in detail in Fig. 9-10. It can be noticed that the most demanding step in the QMSVM is the annealing. The main reason is the high time complexity of the minor embedding algorithm. However, the interesting results are the linear time increase for the solution combination and the constant time for inference with respect to  $N$ . The obtained results are as expected: the solutions combination requires the computation of  $SCMN$  kernels, i.e., it is linear with respect to  $N$ , whereas the classifier used in the inference depends on the  $MC$  problem variables, i.e., it is independent from  $N$ . The outcomes for OVO and CS are also coherent with SVM theory: the training complexity of the Scikit-learn SVM implementation is  $O(N^3)$ , whereas the inference time is linearly dependent on  $N$  [50].

These results clearly show that QMSVM is a much more scalable algorithm with respect to the considered training examples  $N$  compared to standard MSVM methods. Given that the annealing step, which is a fixed step unrelated to  $N$ , has the largest impact in terms of time, the overall execution time can be regarded as near constant.

## V. CONCLUSIONS

QMSVM serves as a preliminary framework for applying QA to a single-step MSVM algorithm, successfully leveraging the D-Wave Advantage quantum annealer in the training step. Although the results show that the prediction accuracy is not higher than standard MSVM algorithms for the same training set, the improved scalability allows the usage of large-scale datasets. Further research has to be conducted, in light of the promising achieved results. Time and accuracy analysis can be performed on different datasets, better assessing the impact of  $N$  and the model parameters on the prediction accuracy. A deeper analysis of different selection methods based on dataset representativeness, on top of the k-means method, can improve the quality of the solutions obtained by the QA. An improvement in performance for QMSVM is expected with the future development of QA, as a higher memory and qubit connectivity allows the usage of a larger training subset and enhances the quality of the obtained solutions.

## ACKNOWLEDGMENT

The authors gratefully acknowledge support from the project JUNIQ that has received funding from the German Federal Ministry of Education and Research (BMBF) and the Ministry

of Culture and Science of the State of North Rhine-Westphalia. This work is part of the Quantum Computing for Earth Observation (QC4EO) initiative from the ESA  $\Phi$ -lab and the Center of Excellence (CoE) Research on AI- and Simulation-Based Engineering at Exascale (RAISE) receiving funding from EU's Horizon 2020 Research and Innovation Framework Programme H2020-INFRAEDI-2019-1 under grant agreement no. 951733. Icelandic HPC National Competence Center is funded by the EuroCC project no. 151454 that has received funding from the EU HPC Joint Undertaking (JU) under grant agreement no. 951732.

## REFERENCES

- [1] M. Chi, A. Plaza, J. A. Benediktsson, Z. Sun, J. Shen, and Y. Zhu, "Big Data for Remote Sensing: Challenges and Opportunities," *Proceedings of the IEEE*, vol. 104, pp. 2207–2219, Nov 2016.
- [2] M. A. Nielsen and I. L. Chuang, *Quantum Computation and Quantum Information: 10th Anniversary Edition*. Cambridge University Press, Dec. 2010.
- [3] R. Jozsa and N. Linden, "On the Role of Entanglement in Quantum-Computational Speed-Up," *Proceedings of the Royal Society of London. Series A: Mathematical, Physical and Engineering Sciences*, vol. 459, pp. 2011–2032, 8 2003.
- [4] T. F. Rønnow, Z. Wang, J. Job, S. Boixo, S. V. Isakov, D. Wecker, J. M. Martinis, D. A. Lidar, and M. Troyer, "Defining and Detecting Quantum Speedup," *Science*, vol. 345, no. 6195, pp. 420–424, 2014. [Online]. Available: <https://www.science.org/doi/abs/10.1126/science.1252319>
- [5] D. Aharonov, A. Kitaev, and N. Nisan, "Quantum Circuits with Mixed States," in *Proceedings of the thirtieth annual ACM symposium on Theory of computing*, 1998, pp. 20–30.
- [6] C. C. McGeoch, *Adiabatic Quantum Computation and Quantum Annealing: Theory and Practice*. Morgan & Claypool Publishers, 2014.
- [7] T. Albash and D. A. Lidar, "Adiabatic Quantum Computation," *Rev. Mod. Phys.*, vol. 90, p. 015002, Jan 2018.
- [8] M. Born and V. Fock, "Beweis des Adiabatsatzes," *Zeitschrift für Physik* 1928 51:3, vol. 51, pp. 165–180, Mar. 1928.
- [9] D. Aharonov, W. van Dam, J. Kempe, Z. Landau, S. Lloyd, and O. Regev, "Adiabatic Quantum Computation is Equivalent to Standard Quantum Computation," *SIAM Review*, vol. 50, no. 4, p. 755–787, 2008.
- [10] T. Kadowaki and H. Nishimori, "Quantum Annealing in the Transverse Ising Model," *Physical Review E*, vol. 58, no. 5, pp. 5355–5363, 1998.
- [11] A. Finnila, M. Gomez, C. Sebenik, C. Stenson, and J. Doll, "Quantum Annealing: A New Method for Minimizing Multidimensional Functions," *Chemical Physics Letters*, vol. 219, no. 5, pp. 343–348, 1994.
- [12] J. Biamonte, P. Wittek, N. Pancotti, P. Rebentrost, N. Wiebe, and S. Lloyd, "Quantum Machine Learning," *Nature*, vol. 549, no. 7671, pp. 195–202, 2017.
- [13] V. Dunjko and H. J. Briegel, "Machine Learning and Artificial Intelligence in the Quantum Domain: a Review of Recent Progress," *Reports on Progress in Physics*, vol. 81, no. 7, p. 074001, jun 2018.
- [14] R. Y. Li, R. D. Felice, R. Rohs, and D. A. Lidar, "Quantum Annealing versus Classical Machine Learning Applied to a Simplified Computational Biology Problem," *npj Quantum Information* 2018 4:1, vol. 4, pp. 1–10, Feb. 2018.
- [15] P. Gawron and S. Lewiński, "Multi-Spectral Image Classification with Quantum Neural Network," in *IGARSS 2020 - 2020 IEEE International Geoscience and Remote Sensing Symposium*, 2020, pp. 3513–3516.
- [16] A. Sebastianelli, D. A. Zaidenberg, D. Spiller, B. L. Saux, and S. L. Ullo, "On Circuit-Based Hybrid Quantum Neural Networks for Remote Sensing Imagery Classification," *IEEE Journal of Selected Topics in Applied Earth Observations and Remote Sensing*, vol. 15, pp. 565–580, 2022.
- [17] S. Otgonbaatar and M. Datcu, "A Quantum Annealer for Subset Feature Selection and the Classification of Hyperspectral Images," *IEEE Journal of Selected Topics in Applied Earth Observations and Remote Sensing*, vol. 14, pp. 7057–7065, 2021.
- [18] —, "Classification of Remote Sensing Images with Parameterized Quantum Gates," *IEEE Geoscience and Remote Sensing Letters*, vol. 19, 2022.
- [19] S. Otgonbaatar, G. Schwarz, M. Datcu, and D. Kranzlmüller, "Quantum Transfer Learning for Real-World, Small, and High-Dimensional Datasets," 2022, arXiv:2209.07799.



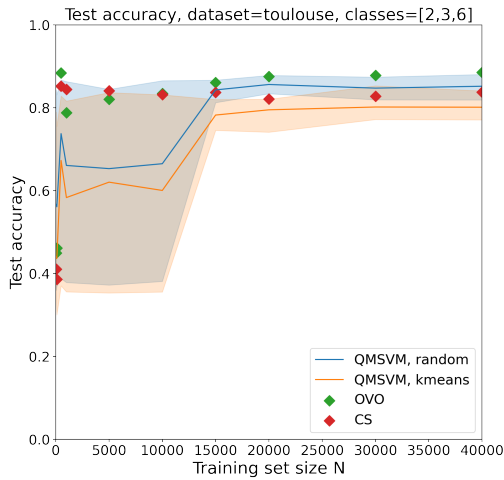
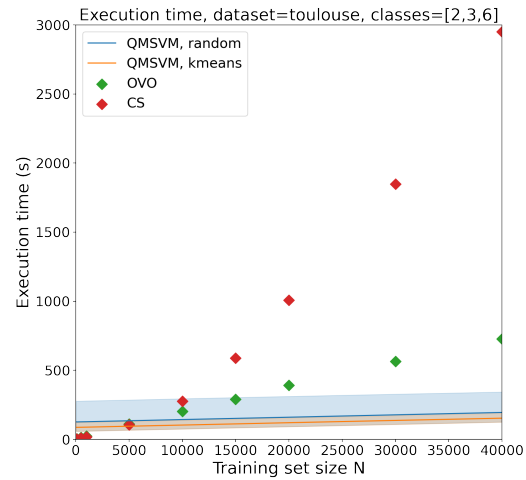
(a) Test accuracy vs. training set size  $N$ (b) Execution time vs. training set size  $N$ 

Fig. 7. Toulouse - test accuracy and execution time for Quantum Multiclass SVM (QMSVM), one-versus-one (OVO) and Crammer-Singer SVM (CS) with respect to training set size  $N$ .

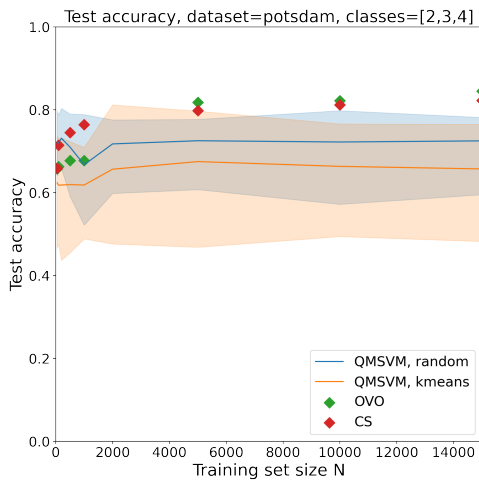
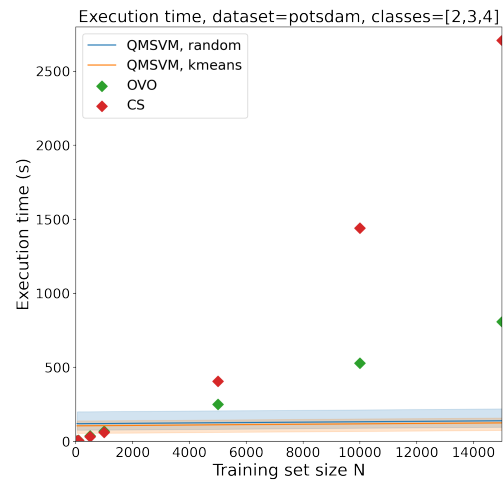
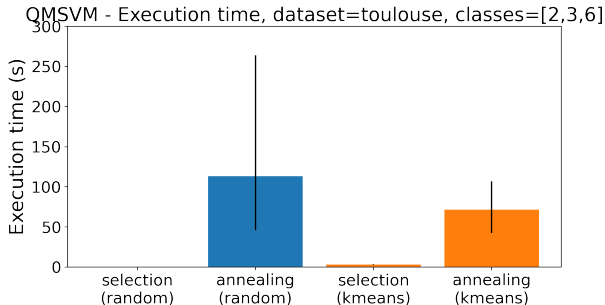
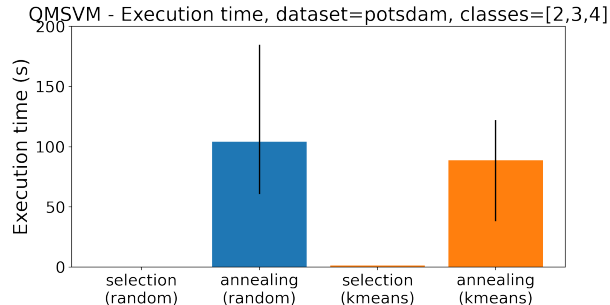
(a) Test accuracy vs. training set size  $N$ (b) Execution time vs. training set size  $N$ 

Fig. 8. Potsdam - test accuracy and execution time for Quantum Multiclass SVM (QMSVM), one-versus-one (OVO) and Crammer-Singer SVM (CS) with respect to training set size  $N$ .

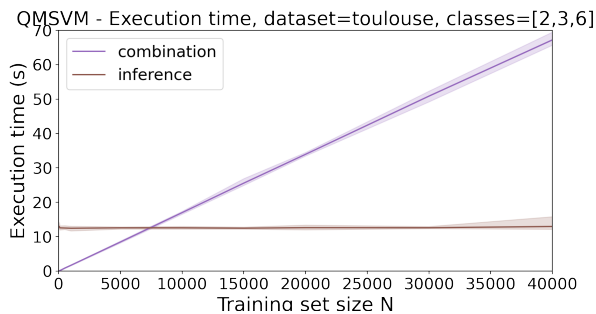
- [20] R. U. Shaik and S. Periasamy, "Accuracy and Processing Speed Trade-offs in Classical and Quantum SVM Classifier Exploiting PRISMA Hyperspectral Imagery," *International Journal of Remote Sensing*, vol. 43, no. 15-16, pp. 6176–6194, 2022.
- [21] A. G. Pai, K. M. Buddhiraju, and S. S. Durbha, "Multiclass Classification of Hyperspectral Remote Sensed Data using QSVC," in *Remote Sensing for Agriculture, Ecosystems, and Hydrology XXIV*, C. M. U. Neale and A. Maltese, Eds., vol. 12262, International Society for Optics and Photonics. SPIE, 2022, p. 122620P.
- [22] S. Huber, K. Glatting, G. Krieger, and A. Moreira, "Quantum Annealing for SAR System Design and Processing," in *EUSAR 2022; 14th European Conference on Synthetic Aperture Radar*, 2022.
- [23] S. Otgonbaatar and M. Datcu, "Quantum Annealer for Network Flow Minimization in InSAR Images," in *EUSAR 2021; 13th European Conference on Synthetic Aperture Radar*, 2021, pp. 1–4.
- [24] —, "Natural Embedding of the Stokes Parameters of Polarimetric Synthetic Aperture Radar Images in a Gate-Based Quantum Computer," *IEEE Transactions on Geoscience and Remote Sensing*, 2021.
- [25] G. Cavallaro, D. Willsch, M. Willsch, K. Michielsen, and M. Riedel, "Approaching Remote Sensing Image Classification with Ensembles of Support Vector Machines on the D-Wave Quantum Annealer," in *Proceedings of the IEEE IGARSS*, 2020, pp. 1973–1976.
- [26] A. Delilbasic, G. Cavallaro, M. Willsch, F. Melgani, M. Riedel, and K. Michielsen, "Quantum Support Vector Machine Algorithms for Remote Sensing Data Classification," in *Proceedings of the IEEE IGARSS*. Institute of Electrical and Electronics Engineers (IEEE), Dec. 2021.
- [27] Y. Ma and G. Guo, *Support Vector Machines Applications*. Springer, 2014, vol. 649.
- [28] F. Melgani and L. Bruzzone, "Classification of Hyperspectral Remote Sensing Images with Support Vector Machines," *IEEE Transactions on*



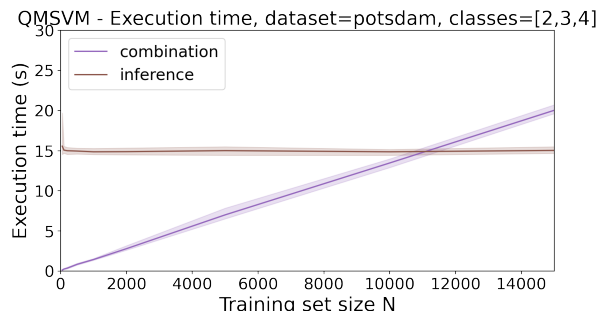
(a) QMSVM (selection, annealing) - Execution time vs. training set size N



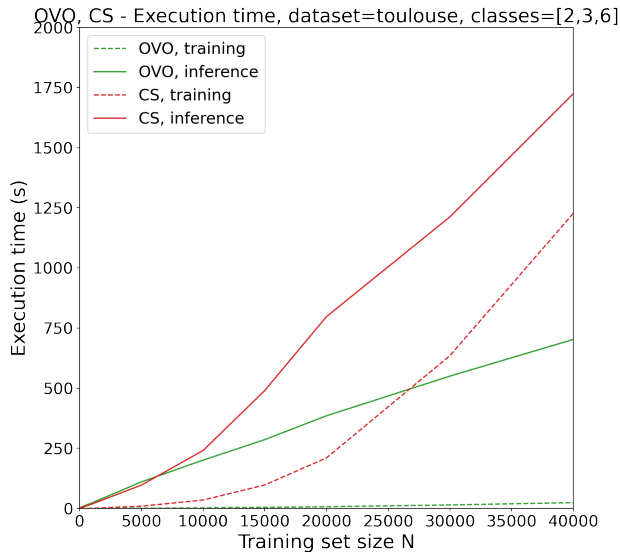
(a) QMSVM (selection, annealing) - Execution time vs. training set size N



(b) QMSVM (combination, inference) - Execution time vs. training set size N

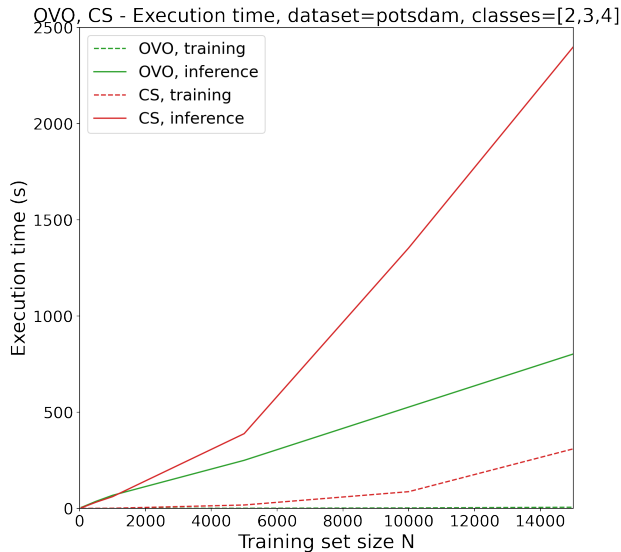


(b) QMSVM (combination, inference) - Execution time vs. training set size N



(c) OVO, CS - Execution time vs. training set size N

Fig. 9. Toulouse - execution time of each performed step, for Quantum Multiclass SVM (QMSVM), one-versus-one (OVO) and Cramer-Singer SVM (CS), with respect to training set size  $N$ .



(c) OVO, CS - Execution time vs. training set size N

Fig. 10. Potsdam - execution time of each performed step, for Quantum Multiclass SVM (QMSVM), one-versus-one (OVO) and Cramer-Singer SVM (CS), with respect to training set size  $N$ .

- Geoscience and Remote Sensing*, vol. 42, no. 8, pp. 1778–1790, 2004.
- [29] C.-W. Hsu and C.-J. Lin, “A Comparison of Methods for Multiclass Support Vector Machines,” *IEEE Transactions on Neural Networks*, vol. 13, no. 2, pp. 415–425, 2002.
- [30] A. K. Bishwas, A. Mani, and V. Palade, “An All-Pair Quantum SVM Approach for Big Data Multiclass Classification,” *Quantum Information Processing*, vol. 17, pp. 1–16, Oct 2018.
- [31] B. A. Dema, J. Arai, and K. Horikawa, “Support Vector Machine for Multiclass Classification using Quantum Annealers,” in *Proceedings of the DEIM Forum*, 2020.
- [32] X.-J. Yuan, Z.-Q. Chen, Y.-D. Liu, Z. Xie, X.-M. Jin, Y.-Z. Liu, X. Wen, and H. Tang, “Quantum Support Vector Machines for Aerodynamic Classification,” 2022, arXiv:2208.07138.
- [33] P. Rebentrost, M. Mohseni, and S. Lloyd, “Quantum Support Vector Machine for Big Data Classification,” *Physical Review Letters*, vol. 113, no. 13, 2014.
- [34] R. Zhang, J. Wang, N. Jiang, H. Li, and Z. Wang, “Quantum Support Vector Machine Based on Regularized Newton Method,” *Neural Networks*, vol. 151, pp. 376–384, 2022.
- [35] V. Havlíček, A. D. Córcoles, K. Temme, A. W. Harrow, A. Kandala, J. M. Chow, and J. M. Gambetta, “Supervised Learning with Quantum-Enhanced Feature Spaces,” *Nature*, vol. 567, no. 7747, pp. 209–212, 2019.
- [36] D. Willsch, M. Willsch, H. D. Raedt, and K. Michielsen, “Support Vector Machines on the D-Wave Quantum Annealer,” *Computer Physics Communications*, vol. 248, Jun 2019.
- [37] K. Crammer and Y. Singer, “On the Algorithmic Implementation of Multiclass Kernel-Based Vector Machines,” *J. Mach. Learn. Res.*, vol. 2, p. 265–292, Mar. 2002.
- [38] D-Wave Systems, <https://www.dwavesys.com/>, accessed: 08/01/2023.
- [39] C. McGeoch and P. Farré, “The Advantage System: Performance Update,” D-Wave Systems, Tech. Rep., 2021.
- [40] P. J. M. van Laarhoven and E. H. L. Aarts, *Simulated Annealing*. Dordrecht: Springer Netherlands, 1987, pp. 7–15.
- [41] J. Cai, W. G. Macready, and A. Roy, “A Practical Heuristic for Finding Graph Minors,” 2014, arXiv:1406.2741.
- [42] R. Roscher, M. Volpi, C. Mallet, L. Drees, and J. D. Wegner, “SemCity Toulouse: a Benchmark for Building Instance Segmentation in Satellite Images,” *ISPRS Annals of Photogrammetry, Remote Sensing and Spatial Information Sciences*, vol. V-5-2020, pp. 109–116, 2020.
- [43] ISPRS, “2D Semantic Labeling Contest - Potsdam,” <https://www.isprs.org/education/benchmarks/UrbanSemLab/2d-sem-label-potsdam.aspx>, accessed: 08/01/2023.
- [44] Forschungszentrum Jülich, <https://www.fz-juelich.de/en/ias/jsc/systems/quantum-computing/juniq-facility/juniq/d-wave-advantagetm-system-jpsi>, accessed: 08/01/2023.
- [45] J. A. Hartigan and M. A. Wong, “Algorithm AS 136: A K-Means Clustering Algorithm,” *Journal of the Royal Statistical Society. Series C (Applied Statistics)*, vol. 28, no. 1, pp. 100–108, 1979.
- [46] D.-S. Huang, K. Li, G. W. Irwin, S.-J. Yen, and Y.-S. Lee, “Under-Sampling Approaches for Improving Prediction of the Minority Class in an Imbalanced Dataset,” *Intelligent Control and Automation*, vol. 344, pp. 731–740, 10 2006.
- [47] F. Pedregosa, G. Varoquaux, A. Gramfort, V. Michel, B. Thirion, O. Grisel, M. Blondel, P. Prettenhofer, R. Weiss, V. Dubourg, J. Vanderplas, A. Passos, D. Cournapeau, M. Brucher, M. Perrot, and E. Duchesnay, “Scikit-learn: Machine Learning in Python,” *Journal of Machine Learning Research*, vol. 12, pp. 2825–2830, 2011.
- [48] T. Joachims, “SVM-Multiclass: Multi-Class Support Vector Machine,” [https://www.cs.cornell.edu/people/tj/svm\\_light/svm\\_multiclass.html](https://www.cs.cornell.edu/people/tj/svm_light/svm_multiclass.html), accessed: 08/01/2023.
- [49] D. Willsch, M. Willsch, C. D. G. Calaza, F. Jin, H. D. Raedt, M. Svensson, and K. Michielsen, “Benchmarking Advantage and D-Wave 2000Q quantum annealers with exact cover problems,” *Quantum Information Processing*, vol. 21, pp. 1–22, 4 2022.
- [50] A. Ns and R. Wardoyo, “Time Complexity Analysis of Support Vector Machines (SVM) in LibSVM,” *International Journal of Computer Applications*, vol. 128, pp. 975–8887, Oct 2015.



machine learning methods for remote sensing applications, with a particular focus on Quantum Computing (QC) and High Performance Computing (HPC).

**Amer Delilbasic** (Student Member, IEEE) received the B.Sc. and M.Sc. degrees in information and communication engineering from the University of Trento in 2019 and 2021, respectively. He is member of the “AI and ML for Remote Sensing” Simulation and Data Lab at the Jülich Supercomputing Centre, Forschungszentrum Jülich, Germany. He is currently pursuing the Ph.D. degree in computational engineering at the University of Iceland. He is an external researcher at  $\Phi$ -lab, European Space Agency, Frascati, Italy. His research interest is mainly in



Learning. He is interested in tackling practical problems that arise in Earth observation, to bring solutions to current environment and population challenges. Dr. Le Saux is an Associate Editor of the *Geoscience and Remote Sensing Letters*. He was Co-Chair (2015–2017) and chair (2017–2019) for the IEEE GRSS Technical Committee on Image Analysis and Data Fusion.

**Bertrand Le Saux** (Senior Member, IEEE) received the Ms.Eng. and M.Sc. degrees from INP, Grenoble, France, in 1999, the Ph.D. degree from the University of Versailles/Inria, Versailles, France, in 2003, and the Dr. Habil. degree from the University of Paris-Saclay, Saclay, France, in 2019. He is a Senior Scientist with the European Space Agency/European Space Research Institute  $\Phi$ -lab in Frascati, Italy. His research interest aims at visual understanding of the environment by data-driven techniques including Artificial Intelligence and (Quantum) Machine



of the joint High Productivity Data Processing research group between the Juelich Supercomputing Centre and the University of Iceland. Since 2020, he is also the EuroHPC Joint Undertaking governing board member for Iceland. His research interests include high-performance computing, remote sensing applications, medicine and health applications, pattern recognition, image processing, and data sciences, and he has authored extensively in those fields. Prof. Dr. – Ing. Morris Riedel online YouTube and university lectures include High-Performance Computing – Advanced Scientific Computing, Cloud Computing and Big Data – Parallel and Scalable Machine and Deep Learning, as well as Statistical Data Mining. In addition, he has performed numerous hands-on training events in parallel and scalable machine and deep learning techniques on cutting-edge HPC systems.

**Morris Riedel** (Member, IEEE) received his PhD from the Karlsruhe Institute of Technology (KIT) and worked in data-intensive parallel and distributed systems since 2004. He is currently a Full Professor of High-Performance Computing with an emphasis on Parallel and Scalable Machine Learning at the School of Natural Sciences and Engineering of the University of Iceland. Since 2004, Prof. Dr. - Ing. Morris Riedel held various positions at the Juelich Supercomputing Centre of Forschungszentrum Juelich in Germany. In addition, he is the Head



methods of quantum phenomena, logical inference approach to quantum mechanics and computational electrodynamics.

**Kristel Michielsen** received her PhD from the University of Groningen, the Netherlands, for work on the simulation of strongly correlated electron systems in 1993. Since 2009 she is group leader of the research group Quantum Information Processing at the Jülich Supercomputing Centre, Forschungszentrum Jülich (Germany) and is also Professor of Quantum Information Processing at RWTH Aachen University (Germany). Her current research interests include quantum computation, quantum annealing, quantum statistical physics, event-based simulation



**Gabriele Cavallaro** (Member, IEEE) received his B.Sc. and M.Sc. degrees in Telecommunications Engineering from the University of Trento, Italy, in 2011 and 2013, respectively, and a Ph.D. degree in Electrical and Computer Engineering from the University of Iceland, Iceland, in 2016. From 2016 to 2021 he has been the deputy head of the “High Productivity Data Processing” (HPDP) research group at the Jülich Supercomputing Centre, Germany. From 2019 to 2021 he gave lectures on scalable machine learning for remote sensing big data at the Institute

of Geodesy and Geoinformation, University of Bonn, Germany. Since 2022, he is the Head of the “AI and ML for Remote Sensing” Simulation and Data Lab at the Jülich Supercomputing Centre, Forschungszentrum Jülich, Germany and an Adjunct Associate Professor with the School of Natural Sciences and Engineering, University of Iceland, Iceland. He is also the Chair of the High-Performance and Disruptive Computing in Remote Sensing (HDCRS) Working Group of the IEEE GRSS ESI Technical Committee and a Visiting Professor at the  $\Phi$ -lab of the European Space Agency (ESA) in the context of the Quantum Computing for Earth Observation (QC4EO) initiative. Since October 2022 he serves as an Associate Editor of the IEEE Transactions on Image Processing (TIP). He also serves on the scientific committees of several international conferences and he is a referee for numerous international journals.

He was the recipient of the IEEE GRSS Third Prize in the Student Paper Competition of the IEEE International Geoscience and Remote Sensing Symposium (IGARSS) 2015 (Milan - Italy). His research interests cover remote sensing data processing with parallel machine learning algorithms that scale on distributed computing systems and cutting-edge computing technologies, including quantum computers.